Chemical Science

ROYAL SOCIETY OF CHEMISTRY

EDGE ARTICLE

View Article Online
View Journal | View Issue

Cite this: *Chem. Sci.*, 2021, **12**, 1886

All publication charges for this article have been paid for by the Royal Society of Chemistry

Received 24th September 2020
Accepted 6th December 2020

DOI: 10.1039/d0sc05277a

rsc.li/chemical-science

Stable monovalent aluminum(I) in a reduced phosphomolybdate cluster as an active acid catalyst†

Ya-Qi Zhang,‡[a] Lai-Yun Zhou,‡[a] Yuan-Yuan Ma,*[a] Kamran Dastafkan,[b] Chuan Zhao,[b] Lan-Zhi Wang*[a] and Zhan-Gang Han*[a]

Low-valent aluminum Al(I) chemistry has attracted extensive research interest due to its unique chemical and catalytic properties but is limited by its low stability. Herein, a hourglass phosphomolybdate cluster with a metal-center sandwiched by two benzene-like planar subunits and large steric-hindrance is used as a scaffold to stabilize low-valent Al(I) species. Two hybrid structures, $(H_3O)_2(H_2bpe)_{11}[Al^{III}(H_2O)_2]_3\{[Al^{I}(P_4Mo_6^{V}O_{31}H_6)_2]_3\cdot 7H_2O$ (abbr. $Al_6\{P_4Mo_6\}_6$) and $(H_3O)_3(H_2bpe)_3[Al^{I}(P_4Mo_6^{V}O_{31}H_7)_2]\cdot 3.5H_2O$ (abbr. $Al\{P_4Mo_6\}_2$) (bpe = *trans*-1,2-di-(4-pyridyl)-ethylene) were successfully synthesized with Al(I)-sandwiched polyoxoanionic clusters as the first inorganic-ferrocene analogues of a monovalent group 13 element with dual Lewis and Brønsted acid sites. As dual-acid catalysts, these hourglass structures efficiently catalyze a solvent-free four-component domino reaction to synthesize 1,5-benzodiazepines. This work provides a new strategy to stabilize low-valent Al(I) species using a polyoxometalate scaffold.

Low- or sub-valence aluminum compounds are increasingly growing into a significant frontier subject in coordination and modern organic synthetic chemistry owing to their unique singlet carbene character, Lewis acid/base properties and catalytic reactivity.[1] However, low-valence aluminum(I) compounds have inherent electron deficiency and exhibit thermodynamic instability, making them prone to self-polymerization with metal–metal bonds[2] or disproportionation[3] to metallic Al and Al(III) species. Inspired by the special stabilizing effect of metallocene compounds, a ligand stabilization strategy has recently been undertaken to stabilize the low-valence aluminum center.[4,5] In this regard, the utilized ligand should satisfy two key criteria: (i) sufficient steric hindrance is required to inhibit monomer polymerization; and (ii) a suitable electronic effect is needed to stabilize the aluminum(I) center. A few organometallic Al(I) compounds protected by bulky organic groups have been prepared such as $[(Cp^*Al)_4]$ ($Cp^* = C_5Me_5$),[6] and $[(CMe_3)_3SiAl_4]$.[7] However, despite having the ligand effect, most of these Al(I) compounds still decompose in aqueous solutions or heating conditions. In contrast to organometallic Al(I) compounds, inorganic Al(I) structures, *i.e.* monomeric monohalides, only exist in gaseous form at high temperature[8] and to the best of our knowledge, no stable inorganic Al(I) compound is known at room temperature due to thermodynamic instability. Therefore, exploring efficient strategies to synthesize stable inorganic Al(I) compounds remains highly desired but a great challenge.

Polyoxometalates (POMs), a diverse family of inorganic molecular clusters based on early-transition metals (W, Mo, V, Nb, and Ta), have extensively attracted attention in research in various fields of materials science, coordination chemistry, medicinal chemistry and catalysis science.[9–11] Owing to their adjustable constituent elements and well-defined structures, POMs have been considered as promising inorganic ligands to stabilize high- and low-valent metal ions. For instance, Rompel *et al.*[12] reported one Keggin-type $[\alpha\text{-}CrW_{12}O_{40}]^{5-}$ anion in which a labile $\{Cr^{III}O_4\}$ tetrahedral unit was assembled at the center of the cluster. Li and co-workers employed a monolacunary Keggin-type inorganic ligand to stabilize a high-valent Cu^{3+} ion.[13] As a unique member of the POM family, the hourglass-type phosphomolybdate cluster $\{M[P_4Mo_6^{V}O_{31}]_2\}^{n-}$ (abbr. $M\{P_4Mo_6\}_2$), consisting of two $[P_4Mo_6^{V}O_{31}]^{12-}$ (abbr. $\{P_4Mo_6\}_2$) subunits bridged by one metal (M) center, represents a fully reduced metal-oxo cluster. With all Mo atoms in the oxidation state of (+5), a more negative charge is endowed to the cluster surface.[14,15] Such high electron density of $\{M[P_4Mo_6^{V}O_{31}]_2\}^{n-}$ polyoxoanions provides an electron-rich local environment for the possible stabilization of unusual-valence metals. It is worth noting that

[a]*Hebei Key Laboratory of Organic Functional Molecules, National Demonstration Center for Experimental Chemistry Education, College of Chemistry and Material Science, Hebei Normal University, Shijiazhuang, Hebei 050024, People's Republic of China. E-mail: mayy334@hebtu.edu.cn; wanglanzhi@126.com; hanzg116@126.com; hanzg116@hebtu.edu.cn*

[b]*School of Chemistry, The University of New South Wales, Sydney, NSW 2052, Australia. E-mail: chuan.zhao@unsw.edu.au*

† Electronic supplementary information (ESI) available. CCDC 1970140 for $Al\{P_4Mo_6\}_2$ and 1970141 for $Al_6\{P_4Mo_6\}_6$. For ESI and crystallographic data in CIF or other electronic format see DOI: 10.1039/d0sc05277a

‡ Y. Q. Zhang and L. Y. Zhou contributed equally to this work.

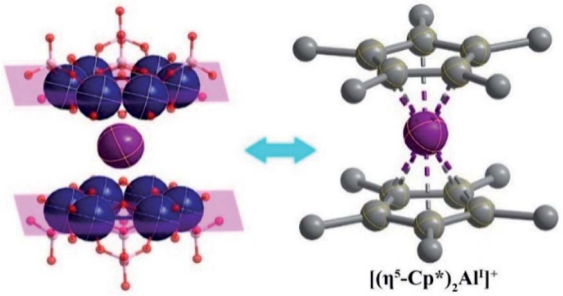

Scheme 1 Similar ferrocene-like sandwich structure features of an inorganic hourglass-type $[Al^I(P_4Mo_6^VO_{31})_2]^{23-}$ polyanion to an organometallic $[(\eta^5\text{-Cp}^*)_2Al^I]^+$ cation.

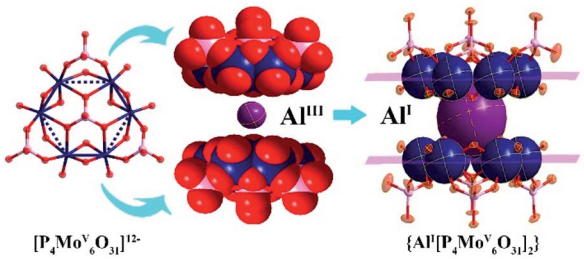

Fig. 1 Ball-and-stick diagram showing the assembly of the hourglass-type cluster $\{Al(P_4Mo_6)_2\}$.

the $[P_4Mo_6^VO_{31}]^{12-}$ subunit presents near-planar triangular structures with the side sizes ranging from 7.50–7.92 Å (Fig. S1†). The structural feature can supply sufficient steric hindrance to restrain the polymerization of low-valence metal species. Moreover, the six Mo atoms in each $[P_4Mo_6^VO_{31}]^{12-}$ subunit arrange in a planar hexagonal-ring structure like a benzene ring, implying that such $\{M[P_4Mo_6^VO_{31}]_2\}^{n-}$ clusters may have a similar delocalized electron structure to conjugated benzene or cyclopentadiene. These features make $[P_4Mo_6^VO_{31}]^{12-}$ a promising candidate with respect to organic protecting groups to construct an inorganic 'ferrocene' analogue of Al(I) (Scheme 1). Therefore, we hypothesize that hourglass-type polyoxoanion clusters are promising to stabilize the labile Al(I) center and isolate inorganic Al(I) species.

Herein, we show a $[P_4Mo_6^VO_{31}]^{12-}$ cluster as an inorganic scaffold to stabilize the Al(I) center in two hybrid compounds, $(H_3O)_2(H_2bpe)_{11}[Al^{III}(H_2O)_2]_3\{[Al^I(P_4Mo_6^VO_{31}H_6)_2]_3\cdot 7H_2O$ (abbr. $Al_6\{P_4Mo_6\}_6$) and $(H_3O)_3(H_2bpe)_3[Al^I(P_4Mo_6^VO_{31}H_7)_2]\cdot 3.5H_2O$ (abbr. $Al\{P_4Mo_6\}_2$) (bpe = *trans*-1,2-di-(4-pyridyl)-ethylene), in which the labile Al(I) center is sandwiched by two $[P_4Mo_6^VO_{31}]^{12-}$ sides, forming an inorganic moiety of a 'ferrocene' analogue. Both $Al_6\{P_4Mo_6\}_6$ and $Al\{P_4Mo_6\}_2$ are experimentally determined at room temperature for the first time, and prepared by hydrothermal reactions of $Na_2MoO_4\cdot 2H_2O$, H_3PO_4, $AlCl_3\cdot 6H_2O$, ethanol and N-containing bpe at 160 °C with slightly different pH values. Notably, the combination of ethanol, N-containing bpe and high hydrothermal temperature is a prerequisite to the isolation of Al(I) species. First, both ethanol and N-containing bpe were used to provide a reducing environment under hydrothermal conditions. By combining high temperature and pressure, sufficient energy is supplied to reduce Mo^{6+} and Al^{3+} ions to Mo^{5+} and Al^+ species, respectively. Then, Mo^{5+} species and phosphoric acid molecules are assembled to form $[P_4Mo_6O_{31}]^{12-}$ subunits, which are subsequently combined with Al^+ ions to form hourglass-type $[Al(P_4Mo_6O_{31})_2]^{23-}$, hence effectively stabilizing Al(I) species (Fig. 1). From the perspective of stereochemistry, two highly negative $[P_4Mo_6O_{31}]^{12-}$ fragments, resembling the methyl cyclopentadiene organic group, sandwich one low-valent metal Al(I) center. Hence, the construction of a strong reducing hourglass-like skeleton makes it possible to stabilize the existing Al^+ species.

Single crystal X-ray diffraction revealed the hourglass-type $\{Al(P_4Mo_6)_2\}$ cluster in $Al_6\{P_4Mo_6\}_6$ and $Al\{P_4Mo_6\}_2$ (Table S1†), in which the $[P_4Mo_6O_{31}]^{12-}$ subunits have a C_3 symmetry and display a near-planar structure formed by six edge-sharing $\{MoO_6\}$ octahedra with alternating short Mo–Mo single bonds and long non-bonding Mo···Mo contacts. The side sizes of the $\{P_4Mo_6\}$ subunit range from 7.50–7.92 Å, which supplies sufficient steric hindrance to restrain the polymerization or disproportionation of low-valence Al(I) species. All Mo atoms are in a reduced oxidation state of +5 and the central Al atoms are in the +1 oxidation state, as confirmed by bond valence calculations (Table S2†). Thus, the synthesized $Al\{P_4Mo_6\}_2$ represents a fully reduced metal–oxygen cluster. Moreover, the six Mo atoms in each $\{P_4Mo_6\}$ subunit present a benzene-like planar hexagonal-ring structure with a similar π-type delocalization electron interaction with Al(I) instead of organic bulky groups. Such π-type delocalization electron interaction constructs an inorganic 'ferrocene' analogue of Al(I) and produces sufficient delocalization energy to stabilize Al(I) species. Considering the formation mechanism of traditional metallocenes, $\{P_4Mo_6\}$ subunits with a similar strong electron-donating ability and suitable steric-hindrance effect on Cp rings, augment the stability of Al(I) species. $Al_6\{P_4Mo_6\}_6$ and $Al\{P_4Mo_6\}_2$ compounds also present the first isolation of aluminum-sandwiched hourglass-type clusters in POM chemistry. Importantly, regarding the inherent and strong hydrolysis of aluminum species in water, these low-valent Al(I)-containing clusters represent the first example of stable solid-state inorganic sub-valent Al(I) compounds at room temperature.

The asymmetric structure of $Al_6\{P_4Mo_6\}_6$ consists of two crystallographically independent $\{Al(P_4Mo_6)_2\}$ clusters sandwiched by central Al(1) and Al(4) atoms, two bridging $[Al(H_2O)_2]^{3+}$ (Al(2) and Al(3)) cations and six protonated bpe cations (Fig. S2†). Aluminum centers involve two kinds of oxidation states: the central Al(1) and Al(4) are in the +1 state, while the bridging Al(2) and Al(3) are in the +3 state. Both Al(1) and Al(4) display the six-coordinated octahedral configuration and bridge two $\{P_4Mo_6\}$ subunits to form two $\{Al^I(P_4Mo_6)_2\}$ clusters. The average lengths of Al–O bonds are 2.318–2.324 Å for Al(1) and Al(4) (Table S3†), which are slightly longer than those of classic Al–O bonds (1.90 Å) for Al(2) and Al(3), but close to that of the Al–O bond in silica-supported alkylaluminum(I) composites.[16–20] The long Al–O lengths for Al(1) and Al(4) centers may be ascribed to the lower electron cloud density located at

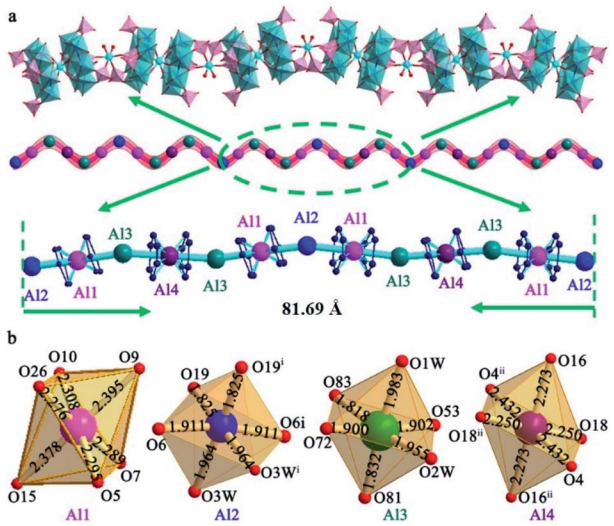

Fig. 2 (a) One-dimensional (1D) inorganic structure in $Al_6\{P_4Mo_6\}_6$ with a length of repeating units of 81.69 Å, consisting of twelve Al-containing fragments ({–Al2–Al1–Al3–Al4–Al3–Al1–Al2–Al1–Al3–Al4–Al3–Al1–}). (b) Four kinds of coordination environments of $\{AlO_6\}$ octahedra, respectively ($i = 1 - x, y, 0.5 - z$; $ii = 0.5 - x, 1.5 - y, 1 - z$).

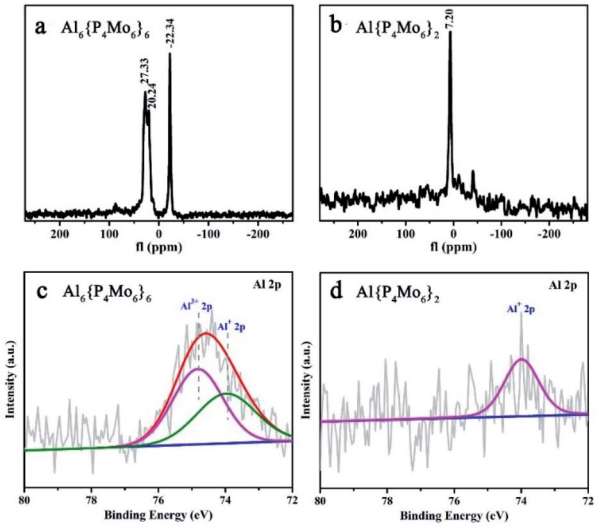

Fig. 3 (a and b) ^{27}Al NMR spectra of solid $Al_6\{P_4Mo_6\}_6$ and $Al\{P_4Mo_6\}_2$; (c and d) XPS spectra of Al in $Al_6\{P_4Mo_6\}_6$ and $Al\{P_4Mo_6\}_2$.

the surface of the Al(I) cation, resulting in slightly longer bonds with the surrounding oxygen donors.[5,21] Moreover, the small distorted extents $(\mathrm{sum}((d_{ij} - d_{ave})/d_{ave})^2/\text{coordination number})$ of $\{Al(1)O_6\}$ (3.86×10^{-4}) and $\{Al(4)O_6\}$ (1.89×10^{-3}) indicate that they are in regular octahedral geometry. Moreover, another structural feature of $Al_6\{P_4Mo_6\}_6$ is that $\{Al^I(P_4Mo_6)_2\}$ clusters are connected by bridging $[Al(H_2O)_2]^{3+}$ cationic fragments (Al(2) and Al(3)), forming an unusual chain-like arrangement (Fig. 2a). It is worth noting that the 1-D chain contains a large repeating monomer with the maximum spacing of 81.69 Å, consisting of twelve Al-containing fragments ({–Al2–Al1–Al3–Al4–Al3–Al1–Al2–Al1–Al3–Al4–Al3–Al1–}). Such a long repeating monomer is rare. Each repeating monomer has two types of symmetric systems: Al(2) in the middle of the monomer plays a center of mirror symmetry and divides the whole repeating monomer into two equidistant half-units of {–Al1–Al3–Al4–Al3–Al1–}; Al(4) in each half-unit further acts as the reverse symmetric center of two {–Al3–Al1–Al2–} subunits. The two types of symmetrical systems form the infinitely extending chain-like structure in $Al_6\{P_4Mo_6\}_6$. Since bpe is a rigid and conjugated molecular structure, an effective $\pi\cdots\pi$ stacking interaction emerges and results in a honeycomb-like supramolecular organic moiety, which accommodates these 1-D inorganic chains and stabilizes the whole $Al_6\{P_4Mo_6\}_6$ framework (Fig. S3 and S4†).

$Al\{P_4Mo_6\}_2$ has a similar structure to $Al_6\{P_4Mo_6\}_6$ (Table S4†), wherein the most obvious difference is that $\{Al^I[P_4Mo_6]_2\}$ clusters exist in isolated form and interact with the surrounding protonated bpe cations *via* hydrogen bonding to form into a 3-D supramolecular framework (Fig. S5 and S6†). The different peripheral environment around the $\{Al^I[P_4Mo_6]_2\}$ cluster can affect its acidity and catalytic activity.

The solid-state ^{27}Al NMR spectrum of $Al_6\{P_4Mo_6\}_6$ depicts two distinct resonances at $\delta = -22.34$ and 27.33 ppm due to the octahedrally coordinated Al^{III} and Al^I sites, respectively (Fig. 3a), indicating two types of Al local environments in $Al_6\{P_4Mo_6\}_6$. In contrast, $Al\{P_4Mo_6\}_2$ displays only one sharp signal at $\delta = 7.20$ ppm due to the octahedrally coordinated Al^I sites (Fig. 3b). The observed narrow peak-width corresponds to the highly symmetric charge distribution at the aluminum nucleus, similar to the ferrocene analogue $[(\eta^5\text{-}Cp^*)_2Al^I]^+$.[5] Noticeably, Al^I resonance in $Al_6\{P_4Mo_6\}_6$ appears at a lower magnetic field compared to $Al\{P_4Mo_6\}_2$, due to the different peripheral environment around the hourglass $\{Al(P_4Mo_6)_2\}$ cluster. XPS spectra of $Al_6\{P_4Mo_6\}_6$ and $Al\{P_4Mo_6\}_2$ further affirm the valence states of Al and Mo elements (Fig. S7 and Table S5†). The Al 2p XPS profile of $Al_6\{P_4Mo_6\}_6$ reveals two peaks at 74.39 and 73.75 eV ascribed to Al^{III} and Al^I, respectively (Fig. 3c). The area ratio of the two peaks is close to 1 : 1, in consistence with the chemical structure of $Al_6\{P_4Mo_6\}_6$. The high-resolution Al 2p XPS spectrum of $Al\{P_4Mo_6\}_2$ displays a weaker broad peak attributed to the low amount of Al^+ (Fig. 3d). Moreover, the structural stabilities of $Al_6\{P_4Mo_6\}_6$ and $Al\{P_4Mo_6\}_2$ were investigated by soaking them in water for 24 hours. Fig. S9–S11† show the comparison of XRD, IR and XPS spectra of $Al_6\{P_4Mo_6\}_6$ and $Al\{P_4Mo_6\}_2$ before and after soaking in water. It can be found that the characteristic diffraction peaks in XRD after soaking for 24 hours still show good agreement with the simulated data (Fig. S9†). The characterized absorption bands in IR spectra also exhibit good match with the original $Al_6\{P_4Mo_6\}_6$ and $Al\{P_4Mo_6\}_2$ (Fig. S10†). The XPS spectra of $Al_6\{P_4Mo_6\}_6$ after soaking in water were also obtained. There is basically no change in the high-resolution spectra of Al 2p with the Al^I/Al^{III} atomic ratios of *ca.* 1 : 1 (Fig. S11†). The spectroscopic and theoretical observations verify that the low valence Al(I) species can stably exist in the reduced phosphomolybdates in the solid state (Fig. S12 and Table S6†). Moreover, the acidities of $Al_6\{P_4Mo_6\}_6$ and $Al\{P_4Mo_6\}_2$ were measured to be 0.27 and

Table 1 Comparison tests of one-pot synthesis of 1,5-benzodiazepine **8aaa** *via* a four-component domino reaction[a]

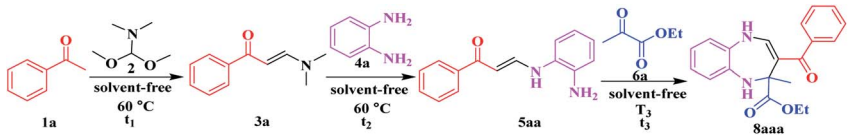

Entry	Catalyst[b]	t_1[f] (h)	Yield[c] (%) **3a**	t_2[f] (h)	Yield[d] (%) **5aa**	T_3 (°C)	t_3[f] (min)	Yield[e] (%) **8aaa**
1	$Al_6\{P_4Mo_6\}_6$	**3.0**	**98**	**1.8**	**92**	**25**	**20**	**83**
2	$Al\{P_4Mo_6\}_2$	3.2	97	2.0	89	25	20	75
3	No catalyst	7.0	98	5.5	62	25	120	Trace
4	*p*-TsOH	4.0	92	3.0	73	25	26	43
5	$AlCl_3$	4.5	94	3.0	82	25	58	29
6	$\{Na[P_4Mo_6]_2\}$	3.5	95	2.5	86	25	30	72

[a] One-pot reaction conditions: acetophenone **1a** (1.00 mmol), *N*,*N*-dimethylformamide dimethyl acetal **2** (1.00 mmol), 1,2-phenylenediamine **4a** (1.00 mmol), ethyl pyruvate **6a** (1.00 mmol) and catalyst (10.00 mg) for the four-component domino reaction. [b] Catalyst (10.00 mg). [c] Isolated yield in the first step. [d] Total isolated yield for the first two steps. [e] Overall isolated yield for the 3 steps. [f] The time taken for the reaction to complete.

0.442 mmol g^{-1}, respectively, demonstrating the promising potential of $Al_6\{P_4Mo_6\}_6$ and $Al\{P_4Mo_6\}_2$ as dual-acid catalysts.

The catalytic performance of $Al_6\{P_4Mo_6\}_6$ and $Al\{P_4Mo_6\}_2$ was evaluated *via* a solvent-free four-component domino reaction for the synthesis of pharmaceutical intermediate 1,5-benzodiazepine (Table 1). With $Al_6\{P_4Mo_6\}_6$ and $Al\{P_4Mo_6\}_2$ as catalysts, the yields of the final product **8aaa** reach 83% and 75%, respectively (Table 1, entries 1 and 2). Almost no **8aaa** is observed without the acid catalysts, even when the reaction is set for a long time (Table 1, entry 3). This clarifies the excellent catalytic performance of $Al_6\{P_4Mo_6\}_6$ and $Al\{P_4Mo_6\}_2$. Typical Brønsted acid *p*-TsOH and Lewis acid $AlCl_3$ as control samples yield only 43% and 29% **8aaa**, respectively (Table 1, entries 4 and 5), much lower than those attained by $Al_6\{P_4Mo_6\}_6$ and $Al\{P_4Mo_6\}_2$ catalysts. Moreover, $(H_2en)_{12}[\{Na_{0.8}K_{0.2}(H_2O)\}_2\{Na[Mo_6O_{12}(OH)_3(HPO_4)_2(PO_4)_2]_2\}_2]\cdot 7H_2O$[22,23] (abbr. $\{Na[P_4Mo_6]_2\}$) in contrast achieved 72% yield of **8aaa** in 30 min, slower than that of $Al_6\{P_4Mo_6\}_6$ and $Al\{P_4Mo_6\}_2$. This indicates the advantage of the unique dual-acid features of Al(III)-stabilized reduced phosphomolybdate clusters with multiple Lewis and Brønsted acid active centers, in which the synergistic effect between the Al species and reduced phosphomolybdate cluster contributes to the catalytic activity.

Furthermore, the $Al_6\{P_4Mo_6\}_6$ catalyst displays a wide substrate scope of auto-tandem catalytic reactions. A series of functional groups including carboxyl, ester and acyl groups on the 2-position of the seven-membered rings can be smoothly converted into the desired 1,5-benzodiazepine products with high and even excellent yields (Table S7†). 1,2-Phenylenediamines 4 which contain both electron-deficient (*p*-Cl and *p*-Br) and electron-rich (*p*-Me and 3,4-di(Me)) 1,2-phenylenediamines also undergo the reaction smoothly, providing the corresponding products in high yields within the given reaction times (Table S7†).

Additionally, the $Al_6\{P_4Mo_6\}_6$ catalyst can be easily recovered by simple filtration. No significant decay in the catalytic activity or selectivity was observed even after 5 recycles of $Al_6\{P_4Mo_6\}_6$ (Fig. S14†). The acquired XRD pattern, and IR and XPS spectra after 5 runs further revealed the good structural integrity and high solid-state stability of $Al_6\{P_4Mo_6\}_6$ (Fig. S15–S17†). Accordingly, the $Al_6\{P_4Mo_6\}_6$ cluster coupled with dual-acid sites presents great potential application towards the four-component domino reaction.

In summary, two cases of low valence Al-centered hourglass-type phosphomolybdates have been reported for the first time. $\{P_4Mo_6\}$ subunits with highly negative charge and a benzene-like planar hexagonal-ring structure, display a similar π-type electron interaction with Al(I) to construct inorganic 'ferrocene' analogues of Al(I), thus effectively stabilizing Al(I) species. Al(I)-POM structures are confirmed and characterized using ^{27}Al NMR and XPS spectra. When used as acid catalysts, both $Al_6\{P_4Mo_6\}_6$ and $Al\{P_4Mo_6\}_2$ efficiently catalyze a solvent-free domino reaction to synthesize 1,5-benzodiazepines with high yield and selectivity. The Al(I)-stabilized reduced POM structures also exhibit excellent substrate compatibility and cycle stability. The design, synthesis and successful stabilization of the subvalent metallic aluminum compounds in the solid state unravel the significance of this study. This work is also important to develop highly active and multifunctional catalysts for organic reactions.

Author contributions

Y. Y. Ma, L. Z. Wang, C. Zhao and Z. G. Han proposed and supervised the project. Y. Y. Ma, L. Z. Wang and Z. G. Han conceived and designed the experiments. Y. Q. Zhang carried out the synthesis and structural characterization of the samples. L. Y. Zhou performed the catalytic experiments. K. Dastafkan, Y. Q. Zhang and L. Y. Zhou co-wrote the original draft. All the authors discussed the results and commented on the manuscript.

Conflicts of interest

There are no conflicts to declare.

Acknowledgements

This work was supported by the National Natural Science Foundation of China (Grants 21871076, 21776060, and 21901060), Natural Science Foundation of Hebei Province (Grants B2016205051, B2020205008 and B2019205074), Natural Science Foundation of Hebei Education Department (Grant BJ2020037) and Graduate Student Innovation Funding Project of Hebei Normal University (CXZZSS2020041). C. Z. is grateful for the award of Future Fellowship from Australian Research Council (FT170100224, DP210103892).

References

1 (*a*) S. G. Gallardo, T. Bollermann and R. A. Fischer, *Chem. Rev.*, 2012, **112**, 3136–3170; (*b*) Y. Liu, J. Li, X. Ma, Z. Yang and H. W. Roesky, *Coord. Chem. Rev.*, 2018, **374**, 387–415; (*c*) A. Dmitrienko, M. Pilkington, J. F. Britten, B. M. Gabidullin, A. Est and G. I. Nikonov, *Angew. Chem., Int. Ed.*, 2020, **59**, 16147–16153; (*d*) S. Grams, J. Eyselein, J. Langer, C. Farber and S. Harder, *Angew. Chem., Int. Ed.*, 2020, **59**, 15982–15986.

2 C. Dohmeier, D. Loos and H. Schnoeckel, *Angew. Chem., Int. Ed. Engl.*, 1996, **35**, 129–149.

3 U. Werner, *Rev. Inorg. Chem.*, 1998, **18**, 239–282.

4 S. Harder and M. H. Prosenc, *Angew. Chem., Int. Ed. Engl.*, 1994, **33**, 1744–1746.

5 C. Dohmeier, H. Schnoeckel, C. Robl, U. Schneider and R. Ahlri-chs, *Angew. Chem., Int. Ed. Engl.*, 1993, **32**, 1655–1657.

6 C. Dohmeier, C. Robl, M. Tacke and H. Schnoeckel, *Angew. Chem.*, 1991, **103**, 594–595.

7 (*a*) C. Schnitter, H. W. Roesky, C. Ropken, R. Herbst-Irmer, H.-G. Schmidt and M. Moltemeyer, *Angew. Chem., Int. Ed.*, 1998, **37**, 1952–1955; (*b*) A. Purath and H. Schnockel, *J. Organomet. Chem.*, 1999, **579**, 373–375; (*c*) C. Cui, H. W. Roesky, M. Noltemeyer, H. G. Schmidt, M. Noltemeyer, H. Hao and F. Cimpoesu, *Angew. Chem.*, 2000, **39**, 4444–4446; (*d*) P. Henke and H. Schnoeckel, *Chem.–Eur. J.*, 2009, **15**, 13391–13398.

8 M. Tacke and H. Schnoeckel, *Inorg. Chem.*, 1989, **28**, 2895–2896.

9 (*a*) S. Omwoma, C. T. Gore, Y. Ji, C. Hu and Y.-F. Song, *Coord. Chem. Rev.*, 2015, **286**, 17–29; (*b*) K. Yu, B. Zhou, Y. Yu, Z. Su, C. Wang, C. Wang, S. Gao and Y. Chen, *Inorg. Chim. Acta*, 2012, **384**, 8–17.

10 (*a*) S. Kim, J. Yeo and W. Choi, *Appl. Catal., B*, 2008, **84**, 148–155; (*b*) Z. Han, X. Xin, R. Zheng and H. Yu, *Dalton Trans.*, 2018, **47**, 3356–3365; (*c*) H. Yang, D. Yang and X. Wang, *Angew. Chem., Int. Ed.*, 2020, **59**, 15527–15531.

11 (*a*) Q. Liu, P. He, H. Yu, L. Gu, B. Ni, D. Wang and X. Wang, *Sci. Adv.*, 2019, **5**, eaax1081; (*b*) Y. Benseghir, A. Lemarchand, M. Duguet, P. Mialane, M. Gomez-Mingot, C. Roch-Marchal, T. Pino, M.-H. Ha-Thi, M. Haouas, M. Fontecave, A. Dolbecq, C. Sassoye and C. Mellot-Draznieks, *J. Am. Chem. Soc.*, 2020, **142**, 9428–9438.

12 N. I. Gumerova, A. Roller, G. Giester, J. Krzystek, J. Cano and A. Rompel, *J. Am. Chem. Soc.*, 2020, **142**, 3336–3339.

13 X. Li, Y. Ren, Z. Weng, B. Yue and H. He, *Chem. Commun.*, 2020, **56**, 2324–2327.

14 (*a*) L. Xu, Y. Sun, E. Wang, E. Shen, Z. Liu, C. Hu, Y. Xing, Y. Lin and H. Jia, *Inorg. Chem. Commun.*, 1998, **1**, 382–385; (*b*) H. Fu, W. Chen, E. Wang, J. Liu and S. Chang, *Inorg. Chim. Acta*, 2009, **362**, 1412–1420.

15 X. Xin, N. Hu, Y. Ma, Y. Wang, L. Hou, H. Zhang and Z. Han, *Dalton Trans.*, 2020, **49**, 4570–4577.

16 Y. Kikukawa, S. Yamaguchi, Y. Nakagawa, K. Uehara, S. Uchida, K. bYamaguchi and N. Mizuno, *J. Am. Chem. Soc.*, 2008, **130**, 15872–15878.

17 C. N. Kato, Y. Makino, M. Yamasaki, Y. Kataoka, Y. Kitagawa and M. Okumura, *Adv. Cryst. Processes*, 2012, **23**, 593–611.

18 Z.-G. Han, X.-Q. Chang, J.-S. Yan, K.-N. Gong, C. Zhao and X.-L. Zhai, *Inorg. Chem.*, 2014, **53**, 670–672.

19 C. Coperet, I. Moroz, P. Florian, J. Viger Gravel, C. P. Gordon and A. Lesage, *Angew. Chem., Int. Ed.*, 2020, **59**, 16167–16172.

20 G. Nikonov, A. Dmitrienko, M. Pilkington, J. F. Britten, B. M. Gabidullin and A. van der Est, *Angew. Chem., Int. Ed.*, 2020, **59**, 16147–16153.

21 D. C. Hutchison, R. D. Stern, L. N. Zakharov, K. A. Persson and M. Nyman, *Inorg. Chem.*, 2020, **59**, 2900–2909.

22 J. Du, Y.-Y. Ma, X. Xin, H. Na, Y.-N. Zhao, H.-Q. Tan, Z.-G. Han, Y.-G. Li and Z.-H. Kang, *Chem. Eng. J.*, 2020, **398**, 125518–125526.

23 X.-R. Tian, L. Hou, J.-J. Wang, X. Xin, H. Zhang, Y.-Y. Ma, Y.-L. Wang, L.-N. Zhang and Z.-G. Han, *Dalton Trans.*, 2018, **47**, 15121–15130.